JJAP Series 7
Mechanisms of Superconductivity 1992, pp. 381–389

Magnetotransport Studies of the Topology of Fermi Surface of the Quasi Two-Dimensional Organic Superconductor $(BEDT\text{-}TTF)_2(NH_4)Hg(SCN)_4$, the Isostructural Metal $(BEDT\text{-}TTF)_2KHg(SCN)_4$, and the Quasi One-Dimensional Superconductor $(TMTSF)_2ClO_4$

Seiichi KAGOSHIMA, Toshihito OSADA, Atsushi KAWASUMI, Ryuta YAGI, Noboru MIURA[1], Masashi OSHIMA[1,*], Hatsumi MORI[2], Toshikazu NAKAMURA[3] and Gunzi SAITO[3]

Department of Pure and Applied Sciences, University of Tokyo, 3-8-1 Komaba, Meguro-ku, Tokyo 153
[1]*Institute for Solid State Physics, University of Tokyo, 7-22-1 Roppongi, Minato-ku, Tokyo 106*
[2]*International Superconductivity Technology Center, 2-4-1 Mutsuno, Atsuta-ku, Nagoya 456*
[3]*Department of Chemistry, Kyoto University, Kitashirakawa-Oiwakecho, Sakyo-ku, Kyoto 606*

(Received December 2, 1991)

Magnetotransport studies are made in the title compounds using magnetic fields up to 40 T. The Fermi surface of BEDT-TTF (bis(ethylenedithiolo)-tetrathiafulvalene) compounds is found to be nearly cylindrical with a weak warping. Its cross-sectional area is estimated as 13–16% of that of the first Brillouin zone. However, unusual features difficult to explain in the current model for this family of compounds are found in $(BEDT\text{-}TTF)_2KHg(SCN)_4$ in the low-temperature-low-field regime below about 8 K and about 22 T. In (TMTSF (tetramethyltetraselenafulvalene))$_2ClO_4$ a clear series of oscillation superposed on the angular dependence of magnetoresistance is found in the metallic and magnetic-field-induced spin-density-wave phases. This new phenomenon is interpreted in terms of a multiple inter-chain transfer.

KEYWORDS: organic superconductor, Fermi surface, magnetoresistance, two-dimensional conductor, one-dimensional conductor

§1. Introduction

$(BEDT\text{-}TTF)_2X$ and $(TMTSF)_2X$ families of organic conductors have attracted much attention because of the electronic low-dimensionality and the possibly strong Coulomb correlation among conduction electrons. Here, BEDT-TTF, TMTSF and X denote bis(ethylenedithiolo)-tetrathiafulvalene, tetramethyltetraselena-fulvalene, and several kinds of anions, respectively. The gapless superconductivity found in both families of compounds[1,2] is considered to be characteristic of a strongly correlated electron system. The spin-density-wave (SDW) found in TMTSF family[3,4] is typical of a low-dimensional electron system having strong Coulomb correlation. For investigations of possible mechanisms of superconductivity in these materials it is necessary to clarify basic structures and properties of electron system.

The purpose of the present study is to find and examine the topology of the Fermi surface and the kinematics of electrons in BEDT-TTF and TMTSF families of compounds by making magnetotransport measurements at low temperatures. Since the Shubnikov-de Haas (SdH) effect was first observed in $(BEDT\text{-}TTF)_2Cu(NCS)_2$,[5] several studies of "fermiology" (Fermi surface topology) of organic conductors have been made to reveal their electronic structures;[6,7] the Shubnikov-de Haas (SdH) effect,[8] and the newly discovered angle-dependent quantum oscillations of magnetoresistance.[6,9] We will employ these methods in the present work.

$(BEDT\text{-}TTF)_2Cu(NCS)_2$, which has polymeric sheets of pseudohalide metal anion $Cu(NCS)_2$, has first exhibited the superconductivity above 10 K.[10] The novel compound $(BEDT\text{-}TTF)_2NH_4Hg(SCN)_4$ and $(BEDT\text{-}TTF)_2KHg(SCN)_4$ to be studied in the present work are synthesized as modifications of $(BEDT\text{-}TTF)_2Cu(NCS)_2$.[11] They have a common layered structure consisting of polymeric sheets of pseudohalide metal anions and donor sheets of zigzag aligned BEDT-TTF molecules which form two-dimensional conducting planes (*ac* planes). In these compounds, a weak interlayer coupling, in other words, strong two-dimensionality is expected since the anion layer thickness is much larger than that of other BEDT-TTF compounds because of a three-dimensional polymeric structure of the anion sheets.

Although $(BEDT\text{-}TTF)_2(NH_4)Hg(SCN)_4$ has a little larger interlayer lattice constant than $(BEDT\text{-}TTF)_2KHg(SCN)_4$ because of the difference of the ion radius between NH_4^+ and K^+, these two compounds are isostructural with each other and their lattice parameter is also nearly the same as each other. Therefore, they are expected to have similar electronic structures.

$(BEDT\text{-}TTF)_2KHg(SCN)_4$ shows metallic behaviors down to 0.5 K with no sign of superconductivity.[11,12] On the other hand, superconductivity with the onset temperature of 1.15 K was recently discovered in $(BEDT\text{-}TTF)_2(NH_4)Hg(SCN)_4$.[13] It is important to study possible origins for the difference of superconducting critical temperature between these isostructural compounds.

In this report we will show that $(BEDT\text{-}TTF)_2KHg(SCN)_4$ has an anomalous state in a low-temperature-low-field regime although it is still open to

*On leave from Japan Carlit Company, Ltd., Shibukawa, Gunma 377.

questions whether this state is responsible for the absence of the superconductivity in this compound.

$(TMTSF)_2X$ has a very simple and typically quasi-one-dimensional electron system. The non-degenerate highest occupied molecular orbital of TMTSF forms one conduction band resulting from the charge transfer with X, so that only a pair of sheet-like open Fermi surfaces is present. The electronic spectrum is well described by a simple tight-binding model with the nearest neighbor transfer integrals along the a, b, and c axes, $t_a:t_b:t_c=300:30:1$. The pair of sheet-like open Fermi surfaces is parallel to the b^*c^* plane (normal to the a axis) with a weak periodic warping due to t_b and t_c. Since t_b is too large to be ignored, the electronic system is usually regarded as an anisotropic two-dimensional one. Standard models for the SDW and the field-induced spin-density-wave (FISDW) are built on this picture that ignores the effect of finite t_c. Really the angular dependence of the threshold field for the FISDW phase obeys a cosine law expected from the two-dimensional model.[14]

On the other hand, the unusual anisotropy of the metallic phase magnetoresistance suggests the three-dimensional nature of the system.[15,16] The angular dependence of the magnetoresistance or the FISDW instability could be affected by this effect.[17,18] Boebinger et al. reported the enhancement of the FISDW structures in the magnetoresistance of $(TMTSF)_2ClO_4$ at the special field angles.[19] Naughton et al. observed several structures having no dependence on the field strength in the magnetoresistance anisotropy in the metallic and FISDW phases.[20]

We will show that these phenomena are explained in terms of a kind of resonance effect for the field direction when the effect of t_c, i.e., the three-dimensionality, is taken into account. It is a commensurability effect (commensurate versus incommensurate) between two periodicities in the electron motion along an open orbit on the Fermi surface warped by t_b and t_c.

Moreover one will see that the magnetotransport properties are understood on the basis of a common model in both BEDT-TTF and TMTSF families in spite of the apparent difference in the shape of the Fermi surface.

§2. Experiments

High-field magnetotransport measurements were made under pulsed magnetic fields up to 40 T generated by a multi-turn solenoid coil. Resistance was measured using an ac bias current (typically $f=200$ kHz, $I_{peak}=1$–0.2 mA) and phase sensitive detection (PSD) to obtain better signal-to-noise ratio. Measurements using low dc bias currents were also done to check the accuracy of the ac measurements and to scale the measured ac data. The angle-dependence of magnetoresistance was measured using a rotating sample holder in static magnetic fields up to 12 T. Temperature was varied in the range 1.5 K–10 K.

In the measurements of $(BEDT\text{-}TTF)_2X$ four gold lead wires (25 μm in diameter) were bonded on both (010) faces (conducting ac plane) of plate-like single crystals by gold paint. The typical sample size was $1\times0.5\times2$ mm^3. Generally, it is difficult to measure the exact in-plane resistance of this kind of materials, since it may contain the interlayer resistance component due to the large anisotropy of conductivity and the irregular sample shape. Therefore, in most of measurements, we measured the inter-layer resistance using the bias current parallel to the b^* axis (perpendicular to the conducting ac plane).

In $(TMTSF)_2ClO_4$ dc magnetoresistance was measured with a current of, typically, 100 μA along the a axis (one-dimensional conducting axis). The typical size of the sample crystals was $4\times0.5\times0.3$ mm^3. The samples were sustained by four leads of gold (25 μm in diameter) bonded by gold paint. To achieve the "relaxed state" with sufficient ordering of the orientation of ClO_4^- anions, the samples were cooled with speeds less than 50 mK/min near the anion ordering transition temperature, 24 K.

§3. Results and Discussions

3.1 *Overall features of the magnetoresistance and the Shubnikov-de Haas effect in $(BEDT\text{-}TTF)_2X$*

3.1.1 *Overall features*

Figure 1 shows the high-field longitudinal magnetoresistance traces at several temperatures under magnetic fields applied perpendicular to the conducting ac plane of $(BEDT\text{-}TTF)_2NH_4Hg(SCN)_4$.[21] The background magnetoresistance increases monotonically with increasing magnetic fields tending to saturate above 10 T. Shubnikov-de Haas (SdH) oscillations are clearly visible above 13 T at 1.5 K. The SdH amplitude grows up rapidly with increasing fields, and reaches 50% of the whole magnetoresistance above 30 T at 1.5 K.

The SdH oscillations are perfectly periodic against inverse magnetic fields as shown in the inset of Fig. 1. The spin splitting of each oscillation peak is not visible in the present temperature and magnetic field ranges. Although the magnetoresistance of the isostructural compound $(BEDT\text{-}TTF)_2KHg(SCN)_4$ shows large decrease and a sharp kink structure after the saturation,[12] this com-

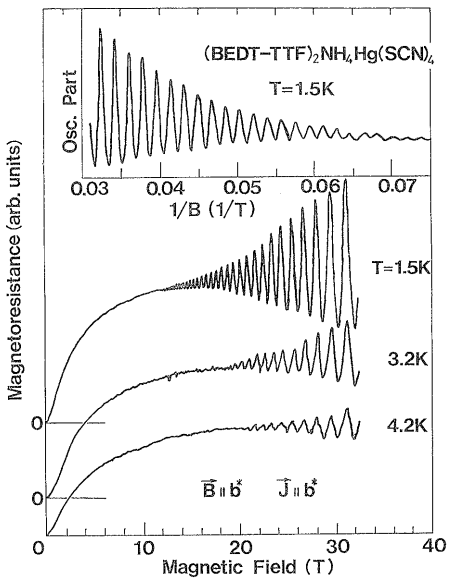

Fig. 1. The longitudinal magnetoresistance of $(BEDT\text{-}TTF)_2(NH_4)Hg(SCN)_4$ at various temperatures under the fields applied perpendicular to the conducting plane. The inset shows the SdH oscillation part as a function of the inverse magnetic fields.

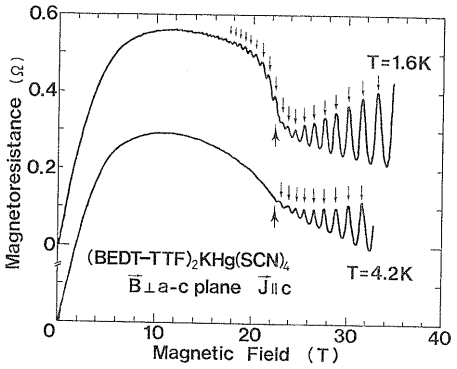

Fig. 2. The transverse magnetoresistance of $(BEDT\text{-}TTF)_2KHg(SCN)_4$ under the fields applied perpendicular to the conducting plane. The kink structure is indicated by the large arrow. The oscillation peaks of the SdH effect are marked by small arrows.

pound shows no anomalous feature in the present field range.

Figure 2 shows an example of the magnetoresistance traces under magnetic fields perpendicular to the conducting plane (*a-c* plane) of $(BEDT\text{-}TTF)_2KHg(SCN)_4$.[12] Although the current direction is almost parallel to the *c*-axis in this case, the measured resistance possibly contains the b^*-axis component because of the irregular sample shape and the large anisotropy of the conductivity. As shown in Fig. 2, the magnetoresistance exhibits remarkable features: With increasing magnetic fields, the magnetoresistance increases sub-linearly and saturates around 10 T. It shows an unusual negative slope above 10 T. A sharp "kink structure" appears around 22.5 T as indicated by large arrows in Fig. 2.

SdH oscillations are also seen superposed on this background magnetoresistance. The amplitude of the SdH oscillations is largely enhanced above the kink structure. The field position of the kink structure shows no explicit temperature-dependence.

The qualitative features mentioned above and the field positions of the kink and the SdH peaks were the same in all the samples although the overall shape of the magnetoresistance trace and the amplitude of the SdH oscillations were slightly sample-dependent. Neither the explicit kink structures nor the SdH oscillations were found when magnetic fields were applied parallel to the *a-c* plane.

3.1.2 *The Shubnikov-de Haas effect*

Temperature dependence of the SdH oscillation amplitude reflects the Landau level spacing. The cyclotron mass mc defined by the Landau level spacing $\hbar eB/m_c$ around the Fermi level is evaluated by numerical fitting of conventional formula for the SdH effect. The Dingle temperature is also obtained from the field dependence of the SdH amplitude using the theoretical formula of the SdH effect in the two-dimensional system. We obtain $m_c/m_0=2.1$ and $T_D=1.4$ K in $(BEDT\text{-}TTF)_2NH_4Hg(SCN)_4$,[21] and $m_c/m_0=1.4$ and $T_D=4.0$ K in $(BEDT\text{-}TTF)_2KHg(SCN)_4$.[12] These values correspond to the relaxation time of $\tau=0.87$ ps and the mean-free path in the conducting plane as $l\sim500$ Å in the former compound, and $\tau=0.3$ ps and $l\sim350$ Å in the latter.

$(BEDT\text{-}TTF)_2NH_4Hg(SCN)_4$ is known to be superconducting below about 1 K while $(BEDT\text{-}TTF)_2KHg(SCN)_4$ is not down to the lowest temperature measured, 0.5 K. It is reasonable that the former compound having the larger cyclotron mass shows the superconductivity, since it has larger density-of-states at the Fermi level. This mass enhancement possibly originates from an increase of the self-energy due to large electron-electron interaction.[22]

The period of SdH oscillations gives the cross-sectional area of the Fermi surface. The period $\Delta(1/B)=0.0018\ T^{-1}$ leads to the area of $S=0.053\ Å^{-2}$ in $(BEDT\text{-}TTF)_2NH_4Hg(SCN)_4$, and $\Delta(1/B)=0.0015\ T^{-1}$ evaluated in $(BEDT\text{-}TTF)_2KHg(SCN)_4$ gives $S=0.065\ Å^{-2}$. These areas correspond to 13% and 16% of the first Brillouin zone of the respective compounds above. We verified that the SdH-oscillation period is dominated by the field component normal to the two-dimensional plane. This is characteristic of the cylindrical Fermi surface that is expected from the two-dimensional structure and the electrical-resistance anisotropy.

Using the above results we discuss basic electronic structures of $(BEDT\text{-}TTF)_2NH_4Hg(SCN)_4$ and $(BEDT\text{-}TTF)_2KHg(SCN)_4$. Since a unit cell contains four BEDT-TTF molecules on the same two-dimensional sheet, two electrons per unit cell are removed from four energy bands made from the BEDT-TTF molecular orbitals. The observed metallic behavior suggests the presence of multiple Fermi surfaces cut by the Brillouin-zone boundary. Mori *et al.* have made a two-dimensional tight-binding band calculation. They show the presence of a closed Fermi surface and a pair of open ones extending nearly parallel to the *c*-axis in the two-dimensional Brillouin zone.[23] The cross-sectional area of the closed Fermi surface is evaluated as about 20% of the area of the first Brillouin zone. This band calculation is semi-quantitatively consistent with the present results.

3.2 *Angle-dependent magnetoresistance and the topology of the Fermi surfaces*

3.2.1 *Warped-cylindrical Fermi surface of $(BEDT\text{-}TTF)_2X$*

Figure 3 shows the dependence of magnetoresistance in $(BEDT\text{-}TTF)_2NH_4Hg(SCN)_4$ on the direction of applied magnetic fields of several fixed strengths. The field direction is measured by the angle θ between the magnetic field

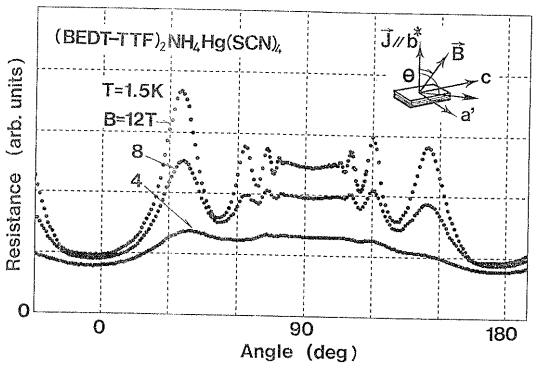

Fig. 3. The angle-dependence of magnetoresistance of $(BEDT\text{-}TTF)_2(NH_4)Hg(SCN)_4$ when the field is tilted from the b^* axis to the $a'+c$ direction at several fixed field strengths.

and the b^* axis (normal to the conducting plane). The magnetic field is tilted from the b^* direction to the $a'+c$ direction (the a' axis is perpendicular to both the b^* axis and the c axis). It is seen that a large angle-dependent oscillation is superposed on the background magnetoresistance having more moderate field dependence. The angle-dependent oscillation appears as a series of peaks and the angle $\theta=0$ is one of the angles of minimum resistance. The oscillation is perfectly periodic against the tangent of the angle θ.

The angle-dependent oscillation of magnetoresistance was discovered in θ-(BEDT-TTF)$_2$I$_3$[9] and β-(BEDT-TTF)$_2$IBr$_2$[6] independently. The angle dependence of magnetoresistance observed in the present experiment is very similar to those observed in the above two compounds.

Yamaji found that this oscillatory phenomenon could be ascribed to the warping of the cylindrical Fermi surface characteristic of two-dimensional electron systems:[24] The energy spectrum of the quasi-two-dimensional system with a weakly warped cylindrical Fermi surface under magnetic fields is composed of a set of Landau subbands with some dispersion along the field direction. When the magnetic field is tilted from the normal to the two-dimensional plane, the Landau-subband width near the Fermi level oscillates against the tilting angle. This leads to an oscillation of conductivity along the field direction because the transport along the field direction is dominated by the Landau subbands.[25] This model is very similar to that for the new type of quantum magnetic oscillations discovered recently in the two-dimensional electron gas formed in a GaAs/Al$_x$Ga$_{1-x}$As heterostructure with a weak lateral periodic potential.[26,27]

Recently, a semi-classical calculation of magnetoresistance was made for this type of Fermi surface using Shockley's tube integral formula.[28] The calculated interlayer magnetoresistance reproduces satisfactorily the observed angle-dependence.

Assuming this model, we can directly obtain the Fermi wave number k_F from the oscillation period for each direction in the two-dimensional plane; $\Delta(\tan\theta)=\pi/bk_F$ in the measurements along principal axes of a Fermi surface's elliptical cross-section. Here b denotes the interlayer spacing.

Our results tell that the cross section of the Fermi surface is nearly circular, and that its radius, k_F is about 0.13 Å^{-1} in (BEDT-TTF)$_2$NH$_4$Hg(SCN)$_4$. This is consistent with the cross-section of the cylindrical Fermi surface evaluated from the Shubnikov-de Haas effect.

In the other compound, (BEDT-TTF)$_2$KHg(SCN)$_4$, we found anomalous features in the angle-dependent magnetoresistance: Figure 4 shows the dependence of magnetoresistance on the direction of the magnetic field measured at several temperatures. The pattern of the angle-dependent oscillation is found to be temperature dependent: Above about 8 K the pattern is similar to that of (BEDT-TTF)$_2$NH$_4$Hg(SCN)$_4$ but in the lower temperature regime it appears to be reversed upside-down. A dip in the high temperature regime turns into a peak in the low temperature one.

Also as functions of the field strength the oscillation

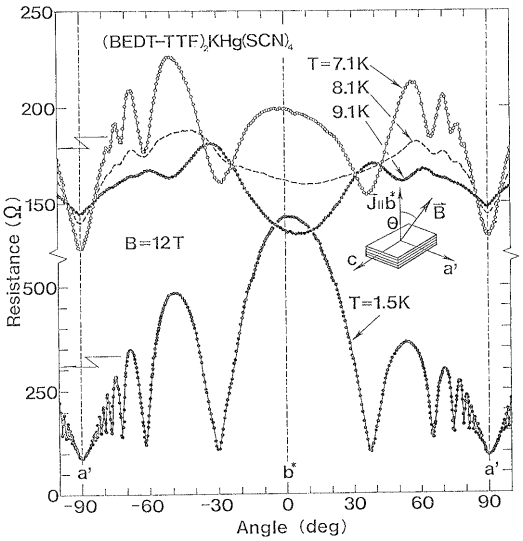

Fig. 4. Angle-dependence of magnetoresistance of (BEDT-TTF)$_2$KHg(SCN)$_4$ measured at several temperatures. The magnetic fields were rotated in the b^*-a' plane.

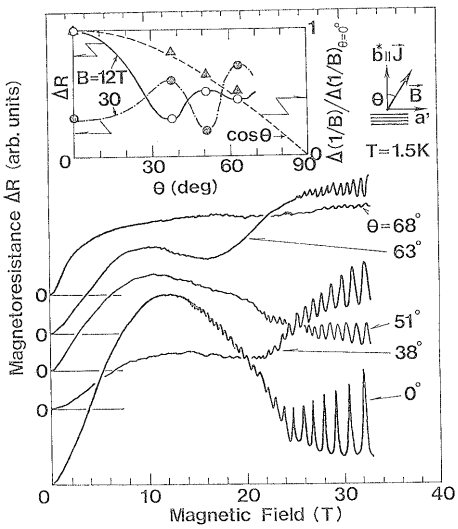

Fig. 5. Field-dependence of magnetoresistance of (BEDT-TTF)$_2$KHg(SCN)$_4$ measured at several tilting angles from the b^* axis. The inset shows the angle dependence derived from these data evaluated at 12 T and 30 T.

pattern changes into the similar one to (BEDT-TTF)$_2$NH$_4$Hg(SCN)$_4$ when the field is higher than about 20 T as shown in Fig. 5.

Thus, one can say that (BEDT-TTF)$_2$KHg(SCN)$_4$ shows anomalous features in the low-temperature-low-field regime below about 8 K and 20 T.

Keeping the above problem in mind, we can tentatively evaluate the Fermi wave number k_F from the oscillation period at the high temperature regime, $k_{Fa}\sim 0.13$ Å^{-1}. It is the same as that of (BEDT-TTF)$_2$NH$_4$Hg(SCN)$_4$ within the experimental error.

It is to be noted, however, the oscillation period of (BEDT-TTF)$_2$KHg(SCN)$_4$ depends on the direction to which the field is tilted from the normal. We found that k_F measured along the c-direction is about a half of that described above, which was measured along the a'-direc-

tion. Therefore the cross-sectional area of the Fermi surface of $(BEDT\text{-}TTF)_2KHg(SCN)_4$ estimated from k_{Fa} and k_{Fc} is a half of that evaluated from the Shubnikov-de Haas effect although these two methods give the same result in the case of $(BEDT\text{-}TTF)_2NH_4Hg(SCN)_4$.

Sasaki *et al.* have found an antiferromagnetic state in the above low-temperature-low-field regime of $(BEDT\text{-}TTF)_2KHg(SCN)_4$.[29] This state may be responsible for the anomalous features found in this compound. We have found, however, no satisfactory explanation to ascribe the anomalies in magneto-transport measurements to the magnetic state. This problem is left for future studies.

3.2.2 *Quasi one-dimensional corrugated Fermi surface of $(TMTSF)_2ClO_4$*

$(TMTSF)_2ClO_4$ is known to be a quasi one-dimensional conductor, whose one-dimensional axis is $\boldsymbol{a}$. For magnetic fields rotated in the ac^* plane, the magnetoresistance anisotropy in the metallic phase almost obeys a cosine law. The c^* component of the magnetic field dominates the magnetoresistance. This is characteristic of quasi one-dimensional conductors.

However, when the magnetic fields are rotated in the b^*c^* plane, which is perpendicular to the conducting $\boldsymbol{a}$ axis, the magnetoresistance shows a large deviation from a cosine law as reported already.[15,16]

Figure 6 shows a plot of the angular dependence of the $\boldsymbol{a}$ axis resistance at 1.5 K for several fixed magnetic fields. The field direction in the b^*c^* plane is measured by the angle θ between the $\boldsymbol{c}^*$ axis and the field direction. At this temperature, the system undergoes the transition from the metallic phase to the field-induced spin-density-wave phase. It occurs with the steep increase of magnetoresistance at the threshold field $B_{th}=6.1$ T under fields along the $\boldsymbol{c}^*$ axis ($\theta=0°$). In Fig. 6, the results in the metallic phase are plotted by closed circles and those in the field-induced spin-density-wave phase by open circles. The threshold angles that separate the metallic phase and the FISDW phase are indicated by large downward arrows. Their positions satisfy the cosine law $B\cos\theta=B_{th}(\theta=0)=6.1$ T as expected for two-dimensional systems.[14]

As is found in the 4 T and 6 T curves in Fig. 6, the resistance in the metallic phase shows the unusual angular dependence deviating from the cosine law: It takes local minima for the fields along the $\boldsymbol{b}'$ ($\theta=90°$) and $\boldsymbol{c}'$ ($\theta=5°$) axes, where $\boldsymbol{b}'$ and $\boldsymbol{c}'$ are the projections of the $\boldsymbol{b}$ and $\boldsymbol{c}$ axes onto the b^*c^* plane. In addition, we find weak dip structures indicated by the small upward arrows at about 48° and 65° in Fig. 6. The position of these fine structures is independent of the strength of magnetic fields. It is contrastive to the threshold structure of the field-induced spin-density-wave transition. The dips at about 48° are considered to be the same ones observed by Boebinger *et al.* and Naughton *et al.*[19,20]

We concentrate on these fine structures of magnetoresistance anisotropy. In addition to the structures marked by arrows, much weaker undulating structures are superposed on the curves in Fig. 6. By taking the second derivative of these curves, one can find these fine structures more clearly as a series of peaks as shown in Fig. 7. The hatched peaks correspond to the threshold for field-induced spin-density-wave and transitions between its subphases. Evidently the positions of the fine structures are independent of the field strength. In addition, even in the FISDW phase the fine structures also appear at the same positions as in the metallic phase.

These facts suggest that the fine structures originate neither from the field-induced spin-density-wave transitions nor from the "fast oscillations" peculiar to $(TMTSF)_2X$,[30] but from some type of topological effect related to the electronic structure.

We find that the fine structures appear when the fractional condition $\tan\theta=1.1\,p/q$ is satisfied, where p and q are integers. Here, we set $p=q=1$ for the largest peak at 48°. In Fig. 7, each peak is labeled by the fraction p/q. The right inset of Fig. 7 shows the tangent of the peak angles plotted against the assigned fraction p/q.

Why does the magnetoresistance show a dip structure at these "magic angles"? The well-known oscillatory

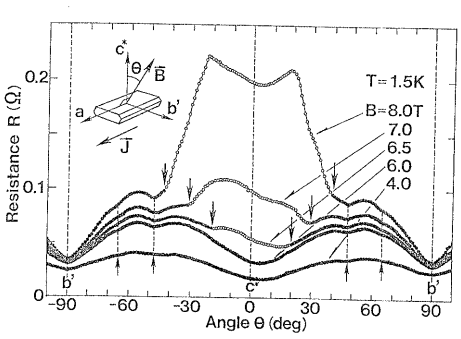

Fig. 6. Magnetoresistance anisotropy of $(TMTSF)_2ClO_4$ at several field values. The filled and open circles stand for the data in the metallic and FISDW phases. The downward and upward arrows indicate the FISDW threshold and the fine structures.

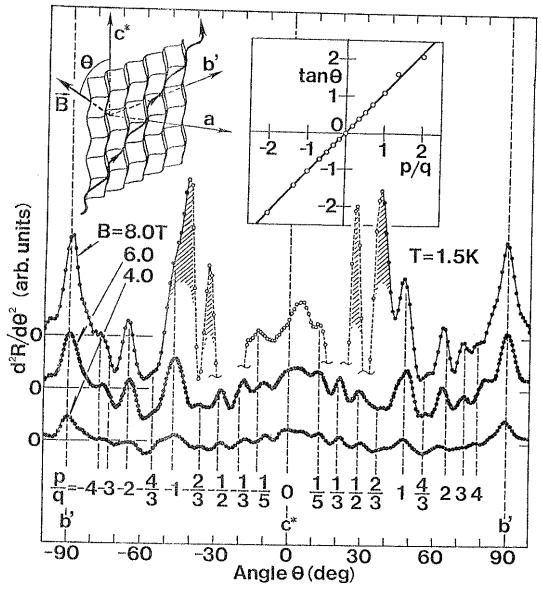

Fig. 7. Second derivative traces of the anisotropy patterns of $(TMTSF)_2ClO_4$ at different field values. The data in the FISDW phase are plotted by the open circles. The hatched peaks correspond to the FISDW transitions. The angles that satisfy $\tan\theta=1.1p/q$ are shown. The right inset shows the plot of the tangent of peak position versusthe fraction p/q. The semiclassical electron motion on the FS is also shown in the left inset.

phenomenon in magnetoresistance anisotropy is observed in the metals having a multiply connected Fermi surface. Another phenomenon is found, as discussed above, in the quasi two-dimensional $(BEDT\text{-}TTF)_2X$ having the warped cylindrical Fermi surface.[6,9] The fine structure found in $(TMTSF)_2ClO_4$ is different from them because $(TMTSF)_2ClO_4$ has only sheet-like Fermi surfaces.

Lebed and Bak have first presented a theory to explain this magnetoresistance anisotropy.[18] Beyond the relaxation time approximation, they estimated the electron relaxation time assuming the following; a three-dimensional band model with two interchain transfer integrals t_b and t_c, and an electron-electron scattering. Their theory could reproduce the overall anisotropy such as local minima for the fields nearly parallel to the b' and the c' axes, but lead to peak structures at magic angles instead of the dip structures observed experimentally.

We propose another model to understand possible origins of local minima and dip structures at the magic angles: We employ the relaxation time approximation and consider the following band model with multiple interchain transfers near the Fermi level of a quasi one-dimensional system.

$$E(\boldsymbol{k})=\hbar v_F(k_x-k_F)-\Sigma_{m,n}t_{mn}\cos(mbk_y+nck_z), \tag{1}$$

where b and c are interchain distances along y and z directions. t_{mn} represents the interchain transfer integral associated with the lattice vector $\boldsymbol{R}_{mn}=(0, mb, nc)$, and $t_{-m-n}=t_{mn}$. Only several t_{mn} with small m and n have finite values and other t_{mn} are negligibly small. The Fermi energy is assumed to be larger than $2\Sigma_{m,n}t_{mn}$, so that there exists a pair of sheet-like open Fermi surfaces perpendicular to the one-dimensional axis (x-axis) as shown in Fig. 8(a).

First, we consider the electronic state under the magnetic fields. Semiclassically, under the magnetic fields, an electron moves along the edge of the Fermi surface cross-section perpendicular to the magnetic field in the $\boldsymbol{k}$ space as shown in Fig. 8(a). It carries out a corresponding orbital motion in the real space as in Fig. 8(b). When a magnetic field $\boldsymbol{B}(0, B\sin\theta, B\cos\theta)$ is applied in the yz-plane perpendicular to the one- dimensional axis, the semiclassical equations of motion, $v=(1/\hbar)\,\mathrm{d}E(\boldsymbol{k})/\mathrm{d}\boldsymbol{k}$, $\hbar(\mathrm{d}\boldsymbol{k}/\mathrm{d}t)=-ev\times\boldsymbol{B}$ lead to

$$v_x(\boldsymbol{k}, t)=\mathrm{sign}(k_x)v_F, \tag{2}$$

$$\begin{pmatrix}v_y(\boldsymbol{k}, t)\\ v_z(\boldsymbol{k}, t)\end{pmatrix}=\sum_{m,n}(t_{mn}/\hbar)\begin{pmatrix}mb\\ nc\end{pmatrix}\times\sin\{G_{mn}x(t)+mbk_y+nck_z\}. \tag{3}$$

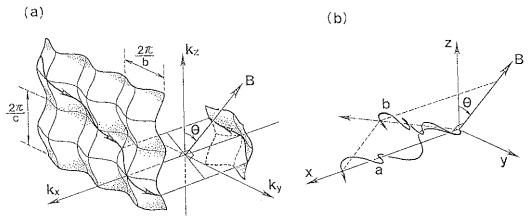

Fig. 8. (a) Sheet-like open Fermi surfaces of the quasi-one-dimensional system in the extended $\boldsymbol{k}$ space. It show the semiclassical electron trajectories when the magnetic field is applied parallel to the lattice vector $\boldsymbol{R}_{12}$. (b) Open orbit motion of the electron in the real space. The orbit b carries the current along the field direction.

Here, $G_{mn}=eB(mb\cos\theta-nc\sin\theta)/\hbar$, $x(t)=\mathrm{sign}(k_x)\,v_Ft$, and $\boldsymbol{k}=(k_x, k_y, k_z)$ is the electron position in the $\boldsymbol{k}$ space at $t=0$.

For general field directions, the electron around the Fermi level carries out an open orbit motion with the velocity v_F along the one-dimensional axis in the real space as the orbit a in Fig. 8(b). This open orbit motion consists of the (m, n) Fourier components oscillating in the $\boldsymbol{R}_{mn}$ direction with the wave number G_{mn} (or the frequency v_FG_{mn}) and the amplitude proportional to $t_{mn}R_{mn}/G_{mn}$. The wave numbers G_{mn} of these components are generally incommensurate to each other.

However, the transverse (y-z) component of v takes a non-oscillatory constant value causing a drifting motion in the x-B plane (x-R_{pq} plane) when the field direction satisfies "the resonant condition,"

$$G_{pq}=0 \quad (\text{or } \tan\theta=pb/qc) \tag{4}$$

for a certain (p, q) with a finite t_{pq}. This means that the open-orbit motion makes the electron drift in the y-z plane when the magnetic field $\boldsymbol{B}$ is parallel to one of the lattice vectors $\boldsymbol{R}_{pq}$ with the finite t_{pq}.

As described below, this motion can carry the electric current along the $\boldsymbol{B}$ direction, causing the resonant increase of the dc longitudinal conduction. For example, the real space orbit b in Fig. 8(b) has a finite average velocity in the $\boldsymbol{B}$ direction in contrast to the orbit a. The wave numbers G_{mn}, where $(m, n)\neq(p, q)$, of the oscillatory (m, n) components of the open orbit are commensurate with each other leading to a periodic open orbit.

This can be described in the quantum mechanical words as the followings. The effective Hamiltonian in the Landau gauge $\boldsymbol{A}=(0, Bx\cos\theta, -Bx\sin\theta)$ is written as

$$H_{\mathrm{eff}}=\hbar v_F(-i\,\mathrm{d}/\mathrm{d}x-k_F)-\Sigma_{m,n}t_{mn}\cos\{G_{mn}x+mb(-i\,\mathrm{d}/\mathrm{d}y)+nc(-i\,\mathrm{d}/\mathrm{d}z)\}. \tag{5}$$

We neglect the Zeeman term. The eigen energy and the envelope function are obtained as

$$E_K=\hbar v_F(K_x-k_F)-\Sigma'_{m,n}t_{mn}\cos(mbK_y+ncK_z), \tag{6}$$

$$F_K(r)=V^{-1/2}\exp\{i\boldsymbol{K}\cdot\boldsymbol{r}+i\,\mathrm{sign}(K_x)\Sigma''_{m,n}(t_{mn}/\hbar v_FG_{mn})\sin(G_{mn}x+mbK_y+ncK_z)\}. \tag{7}$$

where $\boldsymbol{K}=(K_x, K_y, K_z)$ is the quantum number under the magnetic fields. The summation in (6) is taken for (m, n) which satisfies $G_{mn}=0$, and that in (7) is for (m, n) which does not satisfy $G_{mn}=0$. The derivative of the dispersion E_K, i.e., $v_g=(1/\hbar)\mathrm{d}E_K/\mathrm{d}K$ gives the group velocity of the open orbit motion, and it corresponds to the non-oscillatory

part of the semiclassical velocity $\boldsymbol{v}(\boldsymbol{K}, t)$ in (2) and (3).

For general field directions, the spectrum E_K degenerates with respect to K_y and K_z. This means that all the open orbits are equivalent since one trajectory runs through all points on the Fermi surface in the reduced zone scheme. Since E_K depends only on K_x, $\boldsymbol{v_g}$ has only the x-component. This corresponds to the open orbit motion restricted in the x-direction. However, at the field directions satisfying the resonant condition (4), the spectrum has also the K_yK_z-dispersion along the $\boldsymbol{B}$ direction, so that $\boldsymbol{v_g}$ has also a component in the $\boldsymbol{B}$ direction. This means that the electron can move in the x-$\boldsymbol{B}$ plane by the open orbit motion.

The velocity operator $\boldsymbol{v}=(1/\mathrm{i}\hbar)[\boldsymbol{r}, H_{\mathrm{eff}}]$ is given by replacing $x(t)$ with the operator x in (2) and (3). The matrix elements of v_y and v_z connect F_K and $F_{K+G_{mn}}$, where $\boldsymbol{G}_{mn}=(G_{mn}, 0, 0)$, since $\langle \boldsymbol{K}' \exp(\mathrm{i}\,\boldsymbol{G}_{mn}x)\boldsymbol{K}\rangle=\delta_{K',K+G_{mn}}$. At the resonant angles, v_y and v_z have diagonal matrix elements and they coincide with the y and z components of the group velocity $\boldsymbol{v_g}$.

Next, we consider the magnetoconductivity in the quasi one-dimensional system. The complex conductivity is calculated semiclassically by the kinetic form of the Boltzmann equation assuming the constant relaxation time τ,

$$\sigma_{ij}(\omega)=(2e^2/V)\Sigma_k\{-\mathrm{d}f(k)/\mathrm{d}E(k)\}v_i(k,0)v_j(k,t)\,\mathrm{e}^{(1/\tau-i\omega)t}\,\mathrm{d}t, \tag{8}$$

or quantum mechanically by the Kubo-type formula,

$$\sigma_{ij}(\omega)=(-2ihe^2/V)\Sigma_{K,K'}\langle Kv_iK'\rangle\langle K'v_jK\rangle\frac{f(K)-f(K')}{E_{K'}-E_K}\frac{1}{E_{K'}-E_K-\hbar\omega-ih/\tau}. \tag{9}$$

The real part of the complex conductivity elements at low temperatures obtained from (8) or (9) are

$$\sigma_{xx}=N(E_{\mathrm{F}})(ev_{\mathrm{F}})^2\tau/\{1+(\omega\tau)^2\}, \tag{10}$$

$$\begin{pmatrix}\sigma_{yy} & \sigma_{yz}\\ \sigma_{zy} & \sigma_{zz}\end{pmatrix}=N(E_{\mathrm{F}})\sum_{m,n}(et_{mn}/\hbar)^2\begin{pmatrix}m^2b^2 & mnbc\\ mnbc & n^2c^2\end{pmatrix}\frac{\tau}{1+\{(\omega-v_{\mathrm{F}}G_{mn})\tau\}^2}, \tag{11}$$

where $N(E_{\mathrm{F}})=4/2\pi\hbar v_{\mathrm{F}}bc$ is the density of states per unit volume at the Fermi level. The other elements (σ_{xy}, σ_{yx}, σ_{xz}, and σ_{zx}) are zero, so that no Hall effect is expected in the present model. The resistivity along the one-dimensional axis $\rho_{xx}=\sigma_{xx}^{-1}$ shows no field dependence and, therefore, no magnetoresistance. The inter-chain conductivity (11) shows the resonance-like peaks at the frequencies $\omega=v_{\mathrm{F}}G_{mn}$. These peaks correspond to the "open orbit cyclotron resonance".

The dc ($\omega=0$) interchain conductivity is the summation of the tails of these resonances. At the field directions that satisfy the resonant condition (4), one of the resonant frequencies ($v_{\mathrm{F}}G_{pq}$) is zero (dc). Therefore, when B is rotated in the yz-plane, the angular dependence of the dc interchain conductivity shows resonance peaks at the field angles satisfying (4). This resonant increase in the dc conductivity corresponds to the drifting motion of electrons in the B direction only at the field angles satisfying (4).

Conditions for the resonance peak concerning $\boldsymbol{R}_{pq}$ in the dc conductivity to be visible are, (i) the large enough transfer integral t_{pq}, and (ii) the mean free path $v_{\mathrm{F}}\tau$ being larger than the period of the (p, q) component of the open orbit motion:

$$(eBR_{pq}/\hbar)v_{\mathrm{F}}\tau>1. \tag{12}$$

Figure 9 shows an example of the angular dependence of the calculated dc interchain conductivity and resistivity. They are normalized by the z-axis conductivity $\rho_{zz}(0)$ and resistivity $\sigma_{zz}(0)$ at zero magnetic field, respectively. Here, to obtain clear structures, we set $b=c$ and assume the sufficiently large mean free path $Gv_{\mathrm{F}}\tau=(eBb/\hbar)v_{\mathrm{F}}\tau=10$. As for the transfer integrals, we simply set $t_{mn}=1/(m^2/t_b+n^2/t_c)$ for $-5<m, n<5$, where $t_b=t_{10}$

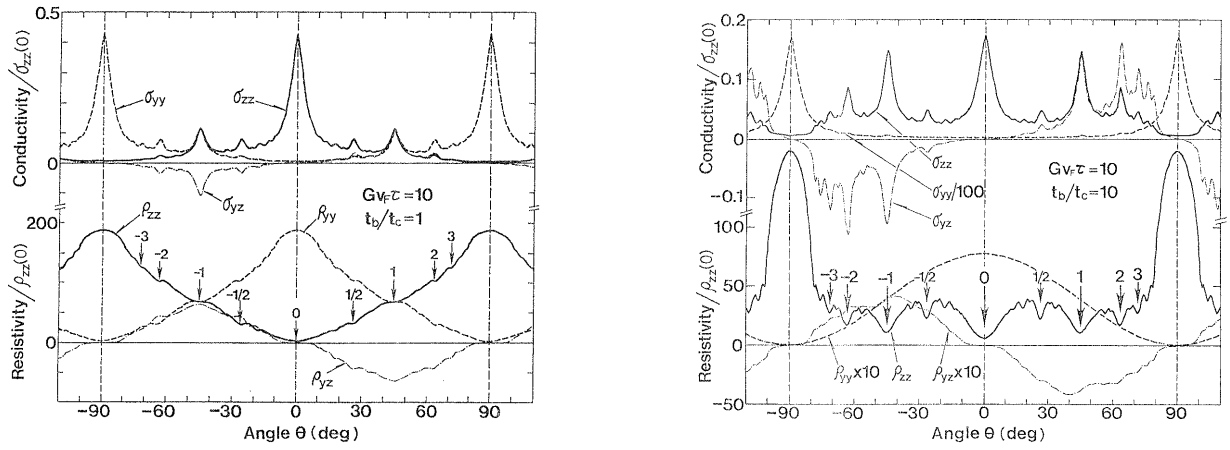

Fig. 9. Calculated dependence of the inter-chain conductivity and resistivity on the magnetic field direction. $t_{mn}=1/(m^2/t_b+n^2/t_c)$, where $t_b=t_{10}$, $t_c=t_{01}$ and $-5<m, n<5$, $Gv_{\mathrm{F}}\tau=(eBb/\hbar)v_{\mathrm{F}}\tau=10$, and $b=c$ were assumed. Dip structures on ρ_{zz} are indicated by arrows and labeled by p/q. (a) Isotropic case ($t_b=t_c$). (b) Anisotropic case ($t_b/t_c=10$).

and $t_c = t_{01}$. The anisotropy in the yz-plane is assumed as $t_b/t_c = 10$.

These assumptions mean that the one-dimensional conducting chains aligned along the y-direction make the conducting layer dominated by the large transfer t_b. These layers are weakly combined by the small interlayer transfers t_c, t_{11}, t_{21}, etc. Compared to the isotropic case, the interlayer transfer integrals t_{11}, t_{21}, $\cdots$ are not so small compared to the nearest neighbor interlayer transfer integral t_c. Since the intralayer transfers t_{m0} do not contribute to the z-axis conductivity σ_{zz}, the resonant structures concerning the interlayer transfers give main contribution to σ_{zz}.

Since $\sigma_{yy} \gg \sigma_{zz}$, $\sigma_{yz}(=\sigma_{zy})$, we obtain $\rho_{zz} = \sigma_{yy}/(\sigma_{yy}\sigma_{zz} - \sigma_{yz}\sigma_{zy}) = 1/\sigma_{zz}$ and $\rho_{zz} \gg \rho_{yy}$, $\rho_{yz}(=\rho_{zy})$. Therefore, on the angular dependence of ρ_{zz}, the resonance-like clear dip structures appear corresponding to the interlayer transfers. On the other hand, the intralayer resistivity ρ_{yy} obeys almost the cosine law, reflecting the large intralayer contribution.

Except the current direction perfectly parallel to the xy-plane, the interlayer resistivity ρ_{zz} gives dominant contribution to the measured resistance because of the large anisotropy of the resistivity $\rho_{zz} \gg \rho_{yy} \gg \rho_{xx}$. In this way, the large anisotropy makes it easy to observe the present resonance effect.

We shall apply this model to the magnetoresistance anisotropy of $(TMTSF)_2X$. We identify the observed local minima and dip structures as the resonant structures discussed above. The transfer integrals between the nearest neighbor TMTSF molecules along the crystal axes have been estimated as $t_a = 300$ meV, $t_b = 30$ meV, and $t_c < 1$ meV.[8] This large anisotropy ($t_b \gg t_c$) is of great advantage to observe the dip structures. The conductivity anisotropy ratio has been reported as $\sigma_a:\sigma_b:\sigma_c = 25:1:10^{-3}$ at $B = 0$.[8] Although the current direction was almost parallel to the a-axis (one-dimensional axis) in the experiments, the measured resistance must contain some interchain components because of the large anisotropy and the irregular sample shape. Really we could obtain a series of much stronger dip structure as expected from the present model by making a direct measurement of the c-axis resistance anisotropy. Thus we consider that the resonance mechanism discussed above is responsible for the observed magnetoresistance anisotropy.

§4. Conclusion

In conclusion, we observed both the large SdH oscillations and the angle-dependent quantum oscillations in the quasi two-dimensional organic superconductor and its family $(BEDT\text{-}TTF)_2(NH_4)Hg(SCN)_4$ and $(BEDT\text{-}TTF)_2KHg(SCN)_4$. The result suggests the strong two-dimensionality and the presence of the cylindrical Fermi surface with weak warping. The cyclotron mass $m_c = 2.1m_0$ of $(BEDT\text{-}TTF)_2NH_4Hg(SCN)_4$ is heavier than that, $m_c = 1.4m_0$, of $(BEDT\text{-}TTF)_2KHg(SCN)_4$ showing no superconductivity. The observed magnetotransport features of the former compound are very "normal" as expected in a typical quasi two-dimensional system, compared to $(BEDT\text{-}TTF)_2KHg(SCN)_4$ that shows anomalous features in the low-temperature-low-field regime below about 8 K and 20 T.

In the quasi one-dimensional superconductor $(TMTSF)_2ClO_4$ we observed fine structures in the magnetoresistance anisotropy as a fractional series of dips in the both metallic and field-induced spin-density wave phases. The field angles of the fine structures obtained experimentally satisfy the fractional condition. They coincide with the magic angles expected from the commensurability condition that the two periods in an open orbit become commensurate.

We find that this phenomenon is ascribed to multiple interchain transfers: The situation is, say, a zero-frequency limit of the "open orbit cyclotron resonance." It is caused by the resonant occurrence of longitudinal conduction by the electron open-orbit motion in the field direction. The appearance of this effect in $(TMTSF)_2ClO_4$ suggests the importance of the three-dimensional nature of this compound.

This picture is common to both the quasi two-dimensional and the quasi one-dimensional conductors studied in the present work. The experimentally observed magnetoresistance is explained in terms of this picture when it is combined with an experimental situation that the largest resistance, i.e., the interlayer or the interchain one, dominates the measured resistance in anisotropic materials.

Acknowledgments

This work is partially supported by a Grant-in-Aid for Scientific Research from the Ministry of Education, Science and Culture, Japan.

References

1) M. Takigawa, H. Yasuoka and G. Saito: J. Phys. Soc. Jpn. **56** (1987) 873.
2) K. Kanoda, K. Akiba, K. Suzuki, T. Takahashi and G. Saito: Phys. Rev. Lett. **65** (1990) 1271.
3) T. Takahashi, Y. Maniwa, H. Kawamura and G. Saito: Physica B **143** (1986) 417.
4) J. M. Delrieu, M. Roger, Z. Toffano, E. Wope Mbougue, R. Saint James and K. Bechgaard: Physica B **143** (1986) 412.
5) K. Oshima, T. Mori, H. Inokuchi, H. Urayama, H. Yamochi and G. Saito: Phys. Rev. B **38** (1988) 938.
6) M. V. Kartsovnik, P. A. Kononovich, V. N. Laukhin and I. F. Shchegolev: Pis'ma Zh. Eksp. Theo. **48** (1988) 498 [JETP Lett. **48** (1988) 541].
7) W. Kang, G. Montambaux, J. R. Cooper, D. Jerome, P. Batail and C. Lenoir: Phys. Rev. Lett. **62** (1989) 2559.
8) See for example, T. Ishiguro and K. Yamaji: "*Organic Superconductors*" (Springer-Verlag, Berlin, 1990).
9) K. Kajita, Y. Nishio, T. Takahashi, W. Sasaki, R. Kato, H. Kobayashi and Y. Iye: Solid State Commun. **70** (1989) 1189.
10) H. Urayama, H. Yamochi, G. Saito, K. Nozawa, T. Sugano, M. Kinoshita, S. Sato, K. Oshima, A. Kawamoto and J. Tanaka: Chem. Lett. (1988) 55.
11) M. Oshima, H. Mori, G. Saito and K. Oshima: Chem. Lett. (1989) 1159.
12) T. Osada, R. Yagi, A. Kawasumi, S. Kagoshima, N. Miura, M. Oshima and G. Saito: Phys. Rev. B **41** (1990) 5428.
13) H. H. Wang, K. D. Carlson, U. Geiser, W. K. Kwok, M. D. Vashon, J. E. Thompson, N. F. Larsen, G. D. McCabe, R. S. Hulsher and J. M. Williams: Physica C **166** (1990) 57.

14) X. Yan, M. J. Naughton, O. S. Cheema, R. V. Chamberlin, S. Y. Hsu, L. Y. Chiang and P. M. Chaikin: Solid State Commun. **66** (1988) 905.
15) R. Brusetti, K. Bechgaard, G. G. Lonzarich and R. H. Friend: J. Phys. (Paris), Colloq. **44** (1983) C3-1055.
16) K. Murata, H. Bando, K. Kajimura, T. Ishiguro, H. Anzai, S. Kagoshima and G. Saito: Mol. Cryst. Liq. Cryst. **119** (1985) 131.
17) A. G. Lebed: Pis'ma Zh. Eksp. Teor. Fiz. **43** (1986) 137 [JETP Lett. **43** (1986) 174].
18) A. G. Lebed and P. Bak: Phys. Rev. Lett. **63** (1989) 1315.
19) G. S. Boebinger, G. Montambaux, M. L. Kaplan, R. C. Haddon, S. V. Chichester, and L. Y. Chiang: Phys. Rev. Lett. **64** (1990) 591.
20) M. J. Naughton, O. H. Chung, L. Y. Chiang and J. S. Brooks: Mat. Res. Soc. Symp. **173** (1990) 257.
21) T. Osada, A. Kawasumi, R. Yagi, S. Kagoshima, N. Miura, M. Oshima, H. Mori, T. Nakamura and G. Saito: Solid State Commun. **75** (1990) 901.
22) N. Toyota, E. W. Fenton, T. Sasaki and M. Tachiki: Solid State Commun. **72** (1989) 859.
23) T. Mori and H. Inokuchi: "*Physics and Chemistry of Organic Superconductors*", ed. G. Saito and S. Kagoshima (Springer-Verlag, Heidelberg, FRG, 1990) p. 204.
24) K. Yamaji: J. Phys. Soc. Jpn. **58** (1989) 1520.
25) T. Osada, R. Yagi, S. Kagoshima, N. Miura, M. Oshima and G. Saito: "*Physics and Chemistry of Organic Superconductors*", ed. G. Saito and S. Kagoshima (Springer-Verlag, Heidelberg, FRG, 1990) p. 220.
26) R. R. Gerhardts, D. Weiss and K. von Klitzing: Phys. Rev. Lett. **62** (1989) 1173.
27) R. W. Winkler, J. P. Kotthaus and K. Ploog: Phys. Rev. Lett. **62** (1989) 1177.
28) R. Yagi, Y. Iye, T. Osada and S. Kagoshima: J. Phys. Soc. Jpn. **59** (1990) 3069.
29) T. Sasaki, H. Sato and N. Toyota: Synthetic Metals **42** (1991) 2211.
30) X. Yan, M. J. Naughton, R. V. Chamberlin, S. Y. Hsu, L. Y. Chiang, J. S. Brooks and P. M. Chaikin: Phys. Rev. B **36** (1987) 1799.